AD-A130 615 A COMPUTER SIMULATION OF THE TIME-DEPENDENT GINZBURG-LANDAU MODEL FOR SPI..(U) CALIFORNIA UNIV SANTA BARBARA DEPT OF CHEMISTRY R PETSCHEK ET AL. 1/1

UNCLASSIFIED MAR 83 TR-6 N00014-81-K-0598 F/G 9/2 NL

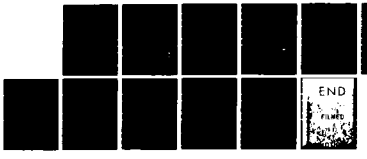

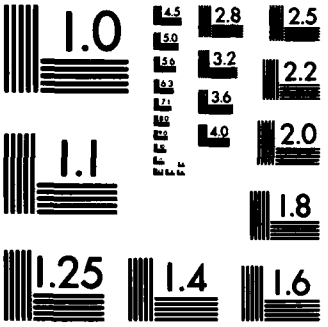

SECURITY CLASSIFICATION OF THIS PAGE (When Data Entered)

(12)

REPORT DOCUMENTATION PAGE

READ INSTRUCTIONS BEFORE COMPLETING FORM

1. REPORT NUMBER	2. GOVT ACCESSION NO.	3. RECIPIENT'S CATALOG NUMBER
6	AD-A130615	

4. TITLE (and Subtitle)

A COMPUTER SIMULATION OF THE TIME-DEPENDENT GINZBURG-LANDAU MODEL FOR SPINODAL DECOMPOSITION

5. TYPE OF REPORT & PERIOD COVERED

Interim Technical Report

6. PERFORMING ORG. REPORT NUMBER

7. AUTHOR(s)

Rolfe Petschek and Horia Metiu

8. CONTRACT OR GRANT NUMBER(s)

N00014-81-K-0598

9. PERFORMING ORGANIZATION NAME AND ADDRESS

University of California
Department of Chemistry
Santa Barbara, CA 93106

10. PROGRAM ELEMENT, PROJECT, TASK AREA & WORK UNIT NUMBERS

NR 056-766/4-21/81 (472)

11. CONTROLLING OFFICE NAME AND ADDRESS

Office of Naval Research
Department of the Navy, Code: 613A:MAC

12. REPORT DATE

March 1983

13. NUMBER OF PAGES

14

14. MONITORING AGENCY NAME & ADDRESS (if different from Controlling Office)

15. SECURITY CLASS. (of this report)

unclassified

15a. DECLASSIFICATION/ DOWNGRADING SCHEDULE

16. DISTRIBUTION STATEMENT (of this Report)

This document has been approved for public release and sale; its distribution is unlimited.

17. DISTRIBUTION STATEMENT (of the abstract entered in Block 20, if different from Report)

18. SUPPLEMENTARY NOTES

Prepared for publication in "Journal of Chemical Physics"
(to appear in November 1983)

19. KEY WORDS (Continue on reverse side if necessary and identify by block number)

20. ABSTRACT (Continue on reverse side if necessary and identify by block number)

In this paper we discuss the results of computer simulations of the time-dependent Ginzburg-Landau equation appropriate to the spinodal decomposition of a two-component mixture with a conserved order parameter. The results for quantities of theoretical interest, such as the probability that the concentration has a particular value in a particular cell, as well as experimentally accessible quantities such as the structure function, are presented. For reasons of computer space, the simulation was done in two dimensions. The effects of incompressible flow, which might be important in some experimental

DD FORM 1473 JAN 73 EDITION OF 1 NOV 65 IS OBSOLETE
S/N 0102-LF 014-6601

SECURITY CLASSIFICATION OF THIS PAGE (When Data Entered)

situations, were not included in these calculations.

OFFICE OF NAVAL RESEARCH

Contract N00014-81-K-0598

Task No. NR 056-766/4-21-81 (472)

Technical Report No. 6

A COMPUTER SIMULATION OF THE TIME-DEPENDENT GINZBURG-LANDAU MODEL FOR SPINODAL DECOMPOSITION

by

Rolfe Petschek and Horia Metiu

Prepared for Publication

in

JOURNAL OF CHEMICAL PHYSICS, November 1983

University of California
Department of Chemistry
Santa Barbara, CA 93106

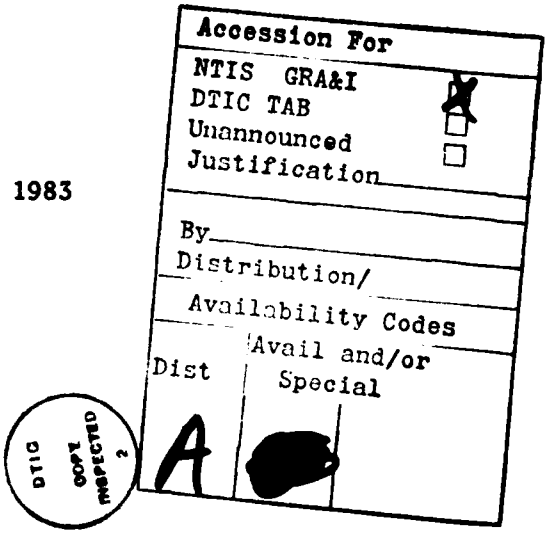

A computer simulation of the time-dependent Ginzburg–Landau model for spinodal decomposition

Rolfe Petschek and Horia Metiu[a)]

Department of Chemistry, University of California, Santa Barbara, California 93106
(Received 27 December 1982; accepted 1 March 1983)

In this paper we discuss the results of computer simulations of the time-dependent Ginzburg–Landau equation appropriate to the spinodal decomposition of a two-component mixture with a conserved order parameter. The results for quantities of theoretical interest, such as the probability that the concentration has a particular value in a particular cell, as well as experimentally accessible quantities such as the structure function, are presented. For reasons of computer space, the simulation was done in two dimensions. The effects of incompressible flow, which might be important in some experimental situations, were not included in these calculations.

I. INTRODUCTION

The term spinodal decomposition is used to describe the process by which a two-component mixture in a thermodynamically unstable region separates into two equilibrium phases.[1–4] This is a process of technological interest since it takes place in alloys,[5] polymers,[6] glasses,[7] and binary liquids.[8] It is also of theoretical interest[9–12] since it provides an example of a far from equilibrium, strongly nonlinear "diffusional" process in which the fluctuations of the order parameter play an important role.

Finally, it is a dynamic process taking place in an unstable phase, below the critical point (we have in mind a phase diagram with an upper critical point), which offers an opportunity to study whether the dynamic scaling laws[13] and the universality behavior observed above T_c in stable phases still hold below T_c under conditions of thermodynamic instability.

A phenomenological theory for the most probable evolution of the concentration during decomposition has been proposed by Chan.[9] This was improved by Cook[10] who added thermal fluctuations. Various reformulations of the Chan–Cook theory were presented by Langer,[11] and Metiu, Kitahara, and Ross.[12]

The phenomenological theory is heuristic and contains a number of approximations whose validity has not been assessed *a priori*:

(a) It is assumed that the probability $P(c(\mathbf{r}), t)$ that the concentration at a point $\mathbf{r}$ has the value $c(\mathbf{r})$ at time t satisfies a master equation[3,11,12] with the transition rate

$$W[c(\mathbf{r}) - c(\mathbf{r}) + \delta c(\mathbf{r})] = \alpha \exp\left\{-\int d\mathbf{r}\, d\mathbf{r}'\, K(\mathbf{r}, \mathbf{r}')\, \delta c(\mathbf{r})\, \delta c(\mathbf{r}')\right\} \times \exp\{-\beta[F(c(\mathbf{r})) + \delta c(\mathbf{r})) - F(c(\mathbf{r}))]/2\}. \quad (1)$$

This is the probability that the concentration changes in unit time from $c(\mathbf{r})$ to $c(\mathbf{r}) + \delta c(\mathbf{r})$. The second exponential in Eq. (1) favors changes which diminish the free energy $F(c)$. The first one introduces a dynamic constraint in the sense that the probability of having an excessively large change $\delta c(\mathbf{r})$ per unit time is very small, even if such a change is strongly favored by the free energy. Even though a theoretical study of the dynamic Ising model[12(b)] showed how one can infer a transition rate of the form taken in Eq. (1), we should consider Eq. (1) to be untested and unproven if extended to other cases such as spinodal decomposition.

(b) If we assume that $K(\mathbf{r}, \mathbf{r}')$ is a number Δ, and that Δ^{-1} is a small parameter, the master equation can be reduced[3,11,12] to the time dependent Ginzburg–Landau equation,

$$\partial c(\mathbf{r}, t)/\partial t = M\nabla^2\, \delta F/\delta c(\mathbf{r}, t) + \eta(\mathbf{r}, t)\,, \quad (2)$$

where M is a kinetic coefficient and $\eta(\mathbf{r}, t)$ is a Gaussian random force satisfying

$$\langle \eta(\mathbf{r}, t)\, \eta(\mathbf{r}, t')\rangle = -2k_B T M\, \delta(t - t')\, \nabla^2\, \delta(\mathbf{r} - \mathbf{r}')\,. \quad (3)$$

The latter requirement is the fluctuation dissipation theorem. Equations (2) and (3) are the Cahn–Cook model for spinodal decomposition. If the reduction of the master equation to the Langevin equation is carried out to a higher order in Δ^{-1}, the resulting equation is rather different from Eq. (3). Furthermore, if Δ^{-1} is not small enough, the reduction cannot be made and we must work with the master equation. There is so far no experimental or theoretical proof that Δ^{-1} is very small; hence that Eq. (2) is adequate for some models of interest.

(c) Finally, all theoretical work has used a van der Waals,[14] Chan–Hilliard,[15] Ginzburg–Landau,[16] Wilson[17] free energy:

$$F(\tau) = (k_B T/2)\int d\mathbf{r}\, [f(c(\mathbf{r})) + K(\nabla c(\mathbf{r}))^2] - F_0 \quad (4a)$$

$$= (k_B T/2)\int d\mathbf{r}\, \{a\, c^2(\mathbf{r}) + (u/2)\, c^4(\mathbf{r}) + K(\nabla c(\mathbf{r}))^2\}\,. \quad (4b)$$

Here $k_B T f(c)/2$ is the free energy density of a uniform system constrained[18] to have the concentration c. Throughout this paper we will use the symbol c to denote the difference between the concentration, denoted

---

[a)] A. P. Sloan Fellow and Camille and Henry Dreyfus, Teacher-Scholar.

by C, and the "critical concentration" and will refer to both loosely as "the concentration." More explicitly c is defined as that variable linear in the actual concentration for which no cubic term appears in the function f. The gradient term takes into account the fact that the free energy is affected by the existence of a spatial inhomogeneity in the concentration field and that the free energy at a given point depends on the concentration at neighboring points. The gradient term stabilizes interfaces between phases and is responsible for surface tension. F_0 is a reference free energy for a homogeneous system. Equation (4b) is obtained from Eq. (4a) by expanding $f(c(\mathbf{r}))$ in power series around the concentration of the homogeneous reference system.

Recent work[13,17,19] has shown that Eq. (4a), and the equation obtained from (4a) and Eq. (2), are a satisfactory starting point for the theory of static and some dynamic critical phenomena. These studies considered, however, only steady-state dynamic phenomena taking place in a stable region of the phase diagram, above the coexistence line and close to the critical point. Therefore their success does not imply that Eqs. (2)–(4) are a satisfactory starting point for a description of spinodal decomposition which takes place in the unstable region below the coexistence line, and is a relaxation experiment following a sudden change in the thermodynamic state which can be carried out far from the critical point.

We consider, therefore, that the assumptions described above are reasonable but, as yet, unproven. Attempts to justify them are hindered by the fact that the competing role of fluctuations, nonlinear interactions, and spatial variation of the order parameter, make these equations extremely difficult to solve. The most ambitious calculations to date are those carried out by Langer, Bar-on and Miller[2] (LBM). These were extended to include hydrodynamic (mode-coupling) effects by Kawasaki and Ohta.[21] An improved LBM type ansatz was recently studied by Hill, Metiu, and Petschek.[22] The method of solution involves heuristic assumptions whose validity is very difficult to assess. We expect[2] that the LBM results are better at the early times of the decomposition process. Further uncertainties in testing these equations are caused by the possibility[23] that the existing data is not free of multiple scattering and, therefore, it should not be compared to single scattering calculations.

Even if the assumptions above are correct the parameters which go into the theory are not generally easy to measure experimentally. Thus it is difficult to make critical comparisons between theory and experiment.

We are thus in a situation in which both the starting equations and their solution might be erroneous, the data are not yet above suspicion and comparisons of theory and experiment are difficul.. For these reasons we have decided that some progress could be made by obtaining the "exact" solution of the time-dependent Ginzburg–Landau equation [Eqs. (2), (3), and (4b)] by a novel type of computer simulation. We can, in principle, test the existing approximate solutions by comparing them to our "exact" results, and we can also compare our calculations to the experiment.

The simulation consists of using finite differences, in time and space, to turn Eq. (2) into an algebraic equation. We program the computer to generate at each "time slice" t_j and spatial point $\mathbf{r}_i$ a random number $\eta(\mathbf{r}_i, t_j)$ taken from a Gaussian distribution whose width is given by the fluctuation–dissipation theorem. We then solve for $c(\mathbf{r}_i, t_j+\Delta t)$ in terms of these random variables and $c(\mathbf{r}_i, t_j)$. We then repeat this procedure until we reach some latest time. A complete run gives us the values of $c(\mathbf{r}_i, t_j)$ at all space points $\mathbf{r}_i$ and times t_j. We call the set $\{c(\mathbf{r}_i, t_j),\ i=1,2,\ldots,\alpha=0,1,2,\ldots\}$ with a "trajectory". If we repeat the calculation we get a second trajectory, which differs from the first one due to stochastic nature of the quantity η. Running many statistically independent trajectories we compute the average value of any function of concentration.

For economic reasons we have carried out such calculations in two dimensions. We report here a variety of quantities: the evolution of the concentration in time during one trajectory; the probability $P_1(c, t)$ that the concentration at a given point, at time t_1, equals c; the probability $P_2(c_i, c_j; t)$ that at time t, the concentration at site i is c_i and that at site j is c_j; the structure factor $S(k, t)$ and its Fourier transform $S(\mathbf{r}, t)$; and some higher moments of $P_1(c_i; t)$.

Since we have carried out two-dimensional calculations we cannot compare directly with three-dimensional experiments. However we show that the simulation reproduces the qualitative features observed in light scattering[3,4]: the scattered light forms a ring which evolves in time so that its intensity grows and its size contracts.

The present theory[5] predicts that if the starting equations have even an approximate validity for physisorbed systems on smooth surfaces [chemisorbed systems can also be simulated if a lattice–molecule potential is added to Eq. (4)], then a binary adsorbed system will undergo at certain concentrations and temperatures, a separation phase transition in which islands of high concentration in one component are formed in a sea of low concentration of the same component. The present calculation describes the rate of island formation. While no kinetic measurements have been made, recent work[25] has shown that the phase diagram of a Ar–Xe mixture on graphite is such that an unmixing process such as spinodal decomposition could occur. This might also happen in intercalated compounds.[26]

Finally we emphasize that the present computer simulation is quite different from previous simulation work which used the Monte Carlo method[27] to study the decomposition in a two-component, nearest neighbor, kinetic Ising model, or used molecular dynamics[28] to study the decomposition of a Lennard-Jones fluid. The connection between these microscopic theories and the Ginzburg–Landau theory used by the phenomenological approach is unclear; the latter must be a coarse grained (in time and space) version of the former models. Furthermore, in the specific case of the Ising model, it is not clear whether the model can be considered a representation of a binary fluid, especially far away from the

critical temperature when universality can no longer be invoked. In the case of molecular dynamics the time scale is of the order of picoseconds, while we are interested in hydrodynamic time scales. Clearly the simulation presented here addresses a different question than previous work, and it is aimed at establishing with accuracy the behavior of the time dependent Ginzburg–Landau model.

II. THE MODEL AND THE METHOD OF SOLUTION

A. The model

Equations (2) and (4a) lead to

$$\partial c(\mathbf{r},t)/\partial t = (k_B T/2)\Delta\Gamma\nabla^2\{\partial f/\partial c(\mathbf{r},t) - K\nabla^2 c(\mathbf{r},t)\} + \eta(\mathbf{r},t)$$
$$= k_B T \Delta\Gamma\nabla^2\left\{\left[a - \frac{K}{2}\nabla^2\right] c(\mathbf{r},t) + u\,c^3(\mathbf{r},t)\right\} + \eta(\mathbf{r},t)\ . \quad (5)$$

Here $c(\mathbf{r},t)$ is the difference between the concentration $C(\mathbf{r},t)$ at the point $\mathbf{r}$ at time t, and the critical concentration C_c. Another important parameter is the concentration c_0 of the system before the quench. If $c_0 \neq 0$ (i.e., off critical quench), it is better to work with $c'(\mathbf{r},t) = c(\mathbf{r},t) - c_0$. When we switch to this new variable, a quadratic term in $c'(\mathbf{r},t)$ appears in Eq. (5). Such a term is thermodynamically necessary since, for example, if $c_0 < 0$ the quadratic term will bias the system towards generating a larger amount of the equilibrium phase having lower concentration. If $c_0 = 0$, the two phases are generated in equal amounts.

If K, u, and η are zero, Eq. (5) reduces to the ordinary diffusion equation. Since $a = (\partial^2 f/\partial^2 c)_{c=c_0}$, $a > 0$ in the thermodynamically stable region of the phase diagram (i.e., above the coexistence line) and the "bare" diffusion coefficient $D_0 = Mk_B Ta$ is positive. If we define the spinodal line by $(\partial^2 f(c)/\partial c^2) = 0$, then the bare diffusion coefficient becomes negative below this line. Equation (5) implies that below the spinodal, if K, u, η are zero, a concentration fluctuation grows spontaneously. This is the kinetic manifestation of the thermodynamic instability.

The gradient term $K|\nabla c|^2$ is introduced into the theory because, as the system becomes spatially inhomogeneous, some free energy must be used to create boundaries between patches having different concentrations. The gradient term accounts for the appearance of a surface tension between such patches. This term prevents the spontaneous growth of the high vector Fourier components $c_k(t)$, since such components result in the formation of sharp domain boundaries with high surface tension.

If $K \neq 0$, but $u, \eta = 0$ (this is Cahn's model[9]), the Fourier transform of the equation gives $\partial c_k(t)/\partial t = -Mk_B T \times k^2(a + Kk^2)\, c_k(t)$ and the Fourier transform of the effective diffusion coefficient is $D(k) = Mk_B T\, k^2(a + Kk^2)$. In the unstable region, where $a < 0$, the Fourier components $c_k(t)$ with $k < \sqrt{|a|/K}$ grow exponentially while the others decay exponentially.

The nonlinear term ($u \neq 0$) becomes mathematically important as the decomposition proceeds and $c(\mathbf{r},t)$ grows. Physically, this is the term which slows down the initial exponential growth of the low k modes. It also contains the thermodynamic information concerning the position, on the phase diagram, of the two final equilibrium phases towards which the system must evolve.

The random force η simulates thermal fluctuations in variables not included in our description. Assuming that they are Gaussian is justified if the system is in local thermodynamic equilibrium and these fluctuations relax quickly.

The form of Eq. (5) is determined by three kinds of assumptions.

(a) If we assume that Δ^{-1} is small, then we can use Eq. (2). To second order in Δ^{-1} the equation for $\partial c/\partial t$ contains[20] additional terms of the form $(\partial F/\partial c)^2$ and $\partial^2 F/\partial c^2$, which are ignored here.

(b) The free energy is a functional of $c(\mathbf{r})$ and the gradient terms $\nabla c \cdot \nabla c$, $\nabla^2 c$, $\nabla^4 c$, etc., which are rotationally and translationally invariant. Equation (4) is an expansion in powers of c and ∇c to the lowest physically reasonable order. All the terms appearing in Eq. (4) are indispensable for a qualitatively correct picture of the decomposition. More terms might be necessary for a quantitatively accurate description.

Above the critical point spatial inhomogeneities are created by thermal fluctuations. Since the phase is thermodynamically stable, the inhomogeneities decay and corresponding concentration fluctuations on large length scales are small. Furthermore, near the critical point the "interfaces" between fluctuations are smooth and $|\nabla c|^2$ tends to be small. This implies that under these conditions Eq. (4) is likely to be quantiatively adequate. This is not, however, certain in spite of the fact that the model has been so successful in explaining both static[19] and dynamic[13,19] critical phenomena. These studies have concentrated on determining the critical exponents, and universality assures that these are not sensitive to the details of the model.

Spinodal decomposition takes place below T_c and the spatial, inhomogeneity is spontaneously created because the system is thermodynamically unstable. Thus $c(\mathbf{r},t)$ grows rapidly and higher powers of c might be necessary in Eq. (4). If the quench is far below T_c there is no *a priori* reason to expect that $(\nabla c)^2$ is small; higher powers of $(\nabla c)^2$ might be needed in Eq. (4) as well.

Note that at early times Eq. (4), and the resulting kinetic Eq. (5), should work well since both c and $\nabla^2 c$ are expected to be small. For this reason it is very important to carry out experiments at the earliest possible times to compare to the theory in a regime in which we expect it to work. If there is some fundamental problem with these equations, more basic than keeping only few terms in the expansion mentioned above, it could show up by producing disagreement with the theory in the short time regime.

(c) A third type of approximation is made by assuming that the concentration is the only relevant field in the problem. In principle, changes in concentration are coupled to changes in energy density (or temperature)

and fluid velocity. In solids, elastic strains which develop during decomposition often play a role.

The hydrodynamic effects have been introduced in the LBM theory by Kawasaki and Ohta.[21] We are currently studying such effects with the present simulation method and hope to report the results in a future article.[31] Hydrodynamic effects are not expected to play a role in alloys, but might be important in binary liquids.

The temperature field has two possible effects. First the temperature and concentration fluctuations are coupled. It is therefore possible that the temperature fluctuations will affect the dynamic behavior of the system (provided it does not relax too quickly). Second if the system relaxes adiabatically the mean temperature of the system will change during the decomposition. This latter effect will be important near the critical point only if the divergent part of the specific heat near the critical point is comparable to the background value of the specific heat. This is true only extremely close to the critical point in typical binary fluids.[32]

B. The method of solution

The time-dependent Ginzburg–Landau equation[5] is a nonlinear, stochastic, partial differential equation. We have approximated it numerically in the following fashion. The order parameter $c(r)$ is given at a discrete set of points on a square lattice. This corresponds to taking a square "Brillouin zone" rather than the circular Brillouin zone favored by theoretical treatments of the time-dependent Ginzburg–Landau equations. This discrete lattice also implies that the underlying point symmetry is only a square symmetry rather than the circular symmetry which would be expected in many systems of physical interest. The largest such lattice used was a square with 32×32 sites, due to limitations in the size of the computer available for this work. The Laplacian was replaced by its finite difference expression

$$h^{2}\nabla^{2}c(x,y) = -4c(x,y)+c(x+h,y)+c(x-h,y) + c(x,y+h)+c(x,y-h)\,, \tag{6}$$

where h is the distance between the centers of two neighboring lattice cells.

This replacement reduces Eq. (5) to a system of $(32)^2$ stochastic, ordinary, differential equations of the form

$$\frac{\partial c(r_i)}{\partial t} = G(\{c(r)\}) + \eta(r_i, t)\,, \tag{7}$$

where G is the finite difference equivalent of the right-hand side of Eq. (5) and $\{c(r)\} = (c(r_1), \ldots, c(r_m))$ with $m = 32\times 32$. This system is solved by writing

$$[c(r, t+\Delta t) - c(r, t)]/\Delta t = G\left(\left\{\tfrac{1}{2}\left(c(r, t+\Delta t) + c(r, t)\right)\right\}\right) + \eta'(r_i, t) \tag{8}$$

with

$$\eta'(r, t) = \int_{t}^{t+\Delta t} \eta(t_1)\, dt_1\,. \tag{9}$$

Using the prescription described below, we generate numerical values for $\eta'(r, t)$. Then we solve Eq. (8) iteratively for $c(r, t+\Delta t)$ [the previous values, $c(r, t)$, is known]. In practice, between two and four iterations were usually sufficient.

The generation of η' has been done as follows. Using the definition Eq. (9) for $\eta'(r, t)$ we compute

$$\langle \eta'(r_1, t_1)\eta'(r_2, t_2)\rangle = -2k_B TM\,\Delta t\,\nabla^2\delta(r_2 - r_1)\,. \tag{10}$$

Using the finite difference expressions for ∇^2 [i.e., Eq. (6)] and the Kroneker delta, δ_{r_1,r_2}, for $\delta(r_1 - r_2)$, find

$$\langle \eta'(r_1, t_1)\,\eta'(r_2, t_2)\rangle = 8\,h^{-2}\,k_B TM\Delta t \tag{aa1}$$

if $r_1 = r_2$ and $t_2 = t_1$,

$$\langle \eta'(r_1, t_1)\,\eta'(r_2, t_2)\rangle = -2\,h^{-2}\,k_B TM\Delta t \tag{11b}$$

if r_1 and r_2 are nearest neighbors and $t_1 = t_2$,

and

$$\langle \eta'(r_1, t_1)\,\eta'(r_2, t_2)\rangle = 0 \tag{11c}$$

otherwise.

This is exactly the form required by the fluctuation–dissipation theorem applied to our discrete system.

Practically we have obtained a Gaussian random field with the covariance given by Eqs. (11) by defining

$$\eta'(x, y, t) = h^{-1}\left[\left(\nu_1(x+h, y, t) - \nu_1(x, y, t)\right) + \nu_2(x, y+h, t) - \nu_2(x, y, t)\right]; \tag{12}$$

here ν_1 and ν_2 are two statistically independent Gaussian fields with the covariance

$$\langle \nu_1(r_1, t_1)\,\nu_1(r_2, t_2)\rangle = \langle \nu_2(r_1, t_1)\,\nu_2(r_2, t_2)\rangle = 2\,k_B TM \tag{13a}$$

if $r_1 = r_2$, $t_1 = t_2$ and

$$\langle \nu_1(r_1, t_1)\,\nu_1(r_2, t_2)\rangle = \langle \nu_2(r_1, t_1)\,\nu_2(r_2, t_2)\rangle = 0 \tag{13b}$$

otherwise.

Note that we need to generate one value of ν_1 and one for ν_2, for each cell of the square lattice [i.e., for each discrete value of the pair (x, y)]. This is accomplished in a standard way by using a packaged generator of uniformly distributed random numbers. In our calculations we have taken the initial concentration to have the same value, c_0, in every cell. This corresponds to the assumption that the initial temperature is so high that there are no fluctuations on the length scales of interest. If the initial temperature were such that the correlation length is comparable to our lattice spacing h it would be necessary to have fluctuations in $c(r, t=0)$. In the appropriate temperature range these fluctuations are approximately Gaussian.

We will assume that the quench is instantaneous. This can be experimentally achieved in binary liquids by using pressure jumps. We are currently studying the behavior of the system under the influence of time dependent temperature (or pressure) changes, etc.

C. The quantities computed

There are a number of quantities that give some insight into the behavior of the decomposing system. The ones computed here are discussed below.

The "one particle" distribution function $P_1(c, t)$ is the probability that the concentration in one cell, at time t, has the value c. We obtain this by making histograms of the values of c at a given time t, for a sufficient number of trajectories. In particular we divide the range of concentrations into which the concentration falls at any given time into a number of evenly spaced intervals. Then for each of the N sites on the lattice and the $\mathfrak{N}$ trajectories we count the number of times, $M(c)$, that the concentration falls into the interval centered on the concentration c. We then estimate the probability as $P_1(c, t) = M(c)\mathfrak{N}^{-1} N^{-1}(\Delta c)^{-1}$, where Δc is the width of the concentration intervals.

The "two particle" distribution function $P_2(c_i', c_j''; t)$ is the probability that, at time t, the concentration in cell i is c_i' and the concentration in cell j is c_j'. This is obtained in a similar way by making histograms for the pair (c_i', c_j') by sampling over all pairs in which the cells have the same geometrical position with respect to each other; the statistics are improved by including in the sampled set values generated by many trajectories.

The structure factor $S(k, t)$ is defined by

$$S_k(t) = \sum_{\alpha=1} \left\{ \sum c_k^*(t)\, c_k(t) \right\}_\alpha N^{-1} \mathfrak{N}^{-1} . \qquad (15)$$

Here

$$c_k(t) = \sum_i c_i(t) \exp(i\mathbf{k} \cdot \mathbf{r}_i) , \qquad (16)$$

where $\mathbf{r}_i$ is the position of the center of the cell i, and $\mathbf{k}$ is the two-dimensional wave vector, constrained to give periodic boundary conditions. That is, $k_x = (2\pi/L)n_x$ and $k_y = (2\pi/L)n_y$, where n_x, n_y are integers. We sum over all the vectors $\mathbf{k}$ having the length k and over all trajectories and divide by the number of trajectories $\mathfrak{N}$ and the number of cells N, to obtain the structure factor per cell.

III. RESULTS AND DISCUSSION

A. The choice of parameters

Except for scale factors, the equilibrium behavior of the Ginzburg–Landau equation depends on two dimensionless parameters. These are the mean field correlation length, given in units of the lattice spacing h, $\xi_{MF} = (|a|/K)^{-1/2} h^{-1}$ and the parameters $G = [(u/4) \times (K/2)^{-d/2}]^{2/(4-d)} (2a)(k_B T)^{-\alpha}$, where d is the dimensionality of the space and $\alpha = d - 1/2(4-d)$. The parameter G is the Ginzburg criterion [see Ref. 19(a), Sec. III 6] which is used to estimate how important the fluctuations are in determining the values of the equilibrium quantities for a system described by Ginzburg–Landau free energy.

For the simulations discussed in this paper we have chosen values $\xi_{MF}^{-2} = 2.5$ ($\xi_{MF} \simeq 0.6$) and $G = 0.2$. Since G is small we expect that the *equilibrium* properties of the system are given, to good approximation, by the mean field theory. Moreover, since the fluctuations are not dominant we do not expect universal behavior.

To establish the importance of the nonlinear effects during the spinodal decomposition we compare the mean square concentration fluctuation given by the linear theory to

$$C_{eq}^2 = [(C_2 - C_1)/2]^2 , \qquad (17)$$

where C_2 and C_1 are the concentrations of the coexisting equilibrium phases at the temperature at which the decomposition takes place. C_{eq} gives us a value of the concentration fluctuation at which we know that nonlinear effects are important. The mean square concentration fluctuations for the linear theory are given by

$$\langle c(r, t)^2 \rangle = \int d\mathbf{k}\, S(k, t)$$

$$\simeq S_{eq}^*(k=0)\,(\xi_{eq}^*/\sqrt{2})^d\, K_d (\tau_0/\pi t)^{1/2} \exp(-t/4\tau_0) , \qquad (18)$$

where $S_{eq}(k=0)$ is the equilibrium value of the structure factor at the temperature $T^* = T_c + |\Delta T|$ (ΔT is the magnitude of the temperature quench $T_c - T$, where T is the temperature at which the decomposition takes place), $K_d = 2^{-d+1}\pi^{-d/2}\Gamma(d/2)^{-1}$ is the area of a d-dimensional surface[19(a)] divided by $S^*(k=0)$, ξ^* is the correlation length at the temperature T^* and

$$\tau_0 = K/2Ma \qquad (19)$$

is the decomposition time scale for the linear theory (one-quarter the growth rate of the growing mode). The last term in Eq. (18) is the asymptotic (long time) value of the integral.

Thus we see that the length of time during which the linear theory is applicable is given (in units of τ_0) by the logarithm of

$$R = C_{eq}^2 (\xi^*/\sqrt{2})^d / [S_{eq}^*(k=0)\, K_d] . \qquad (20)$$

For the parameter values used in the present simulations, the value of R is 10 (in computing this we used mean field values for ξ^*, S_{eq}^*, C_2, and C_1. As the experimental[22] (and theoretical) value of R in three dimensions is 16 we expect the effect of the nonlinearity in the present simulation to be comparable to that in three dimensions near the critical point.

The initial concentration in all the simulations presented here was taken to be the same in all cells. This implies that the system is initially at a temperature high above the critical point so that the initial fluctuations are very small compared to those occurring during spinodal decomposition. In one simulation the initial concentration was taken to have its critical value, so that $c(t=0) = 0$. In the other we use $c(t=0) = -0.47 C_{eq}$ (with C_{eq} as defined in Eq. (18), computed within mean field Ginzburg–Landau theory).

B. Results

1. *The concentration pattern and its growth*

Figures 1 and 2 show qualitatively the concentration patterns generated by one trajectory, at three different times following the quench. The darkness in a given cell is roughly proportional to the concentration therein. The darkest cells have the largest positive deviation of the concentration from the critical value, and the lightest ones have the largest negative deviation. In the off critical quench (Fig. 2) the cells having the majority

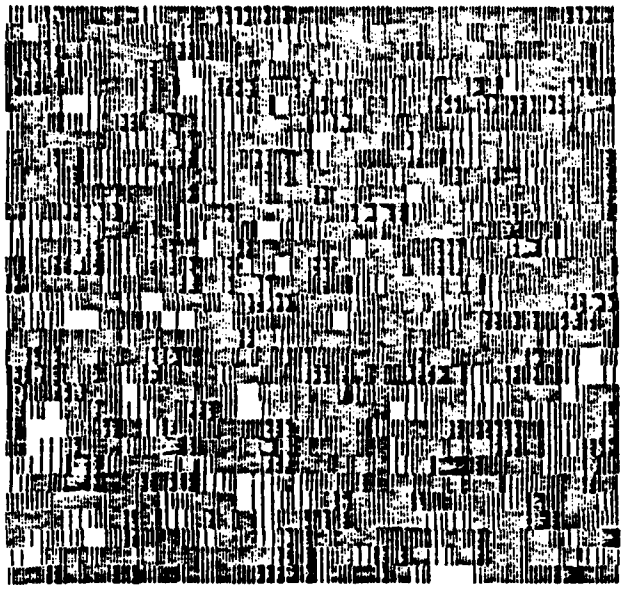

(a)

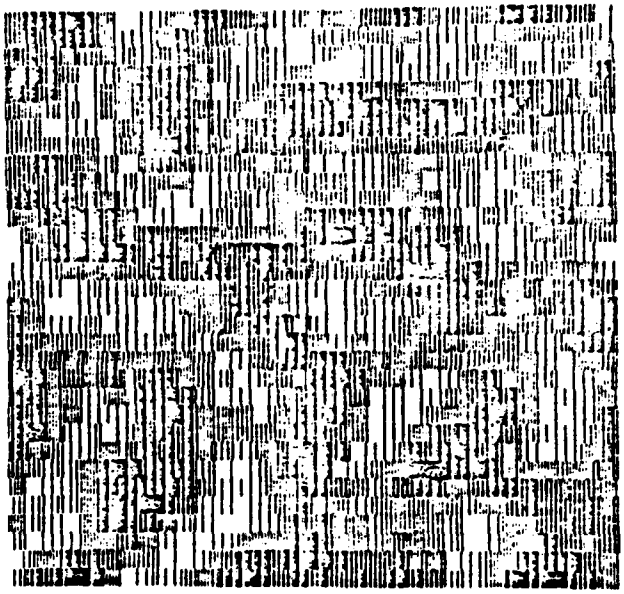

(b)

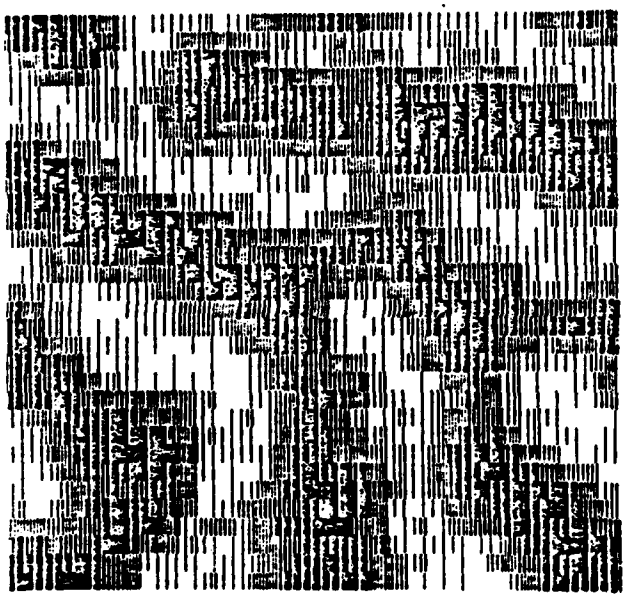

(c)

FIG. 1. This figure gives a qualitative visual impression of the concentration distribution during spinodal decomposition, in critical quench. The degree of darkness is proportional to the local concentration. The light (dark) squares are placed where the local concentration is smaller (larger) than the critical concentration. The Figs. (a), (b), and (c) represent the concentration distribution at the times 10 τ_0, 56 τ_0, and 223 τ_0, respectively, after the quench. The darkness scale has been chosen so that the lightest and the darkest squares represent places where $c \sim 1.1\, C_{eq}$, that have the maximum concentration fluctuations. The mean field value of C_{eq} [defined in Eq. (17)] was used.

phase concentration are colored lightly. Note that as the size of the concentration patches increases the boundary between them becomes sharper.

2. *The structure factor and other moments*

In Fig. 3 we have shown typical plots of the dimensionless structure factor per unit cell, $K\langle|c(k)|^2\rangle/N k_B T$, where N is the number of lattice sites and K is defined in Eq. (4a). The structure function S has been plotted as a function of $|k|' = [4 - 2(\cos(k_x h) + \cos(k_y h))]^{-1/2}$, the discrete analog of the magnitude of k. In particular, $|k|'$ is simply the square root of the Fourier transform of the discrete Laplacian [Eq. (6)]. It has been made dimensionless by multiplying by the lattice spacing h. It is essentially identical to the usual definition of the magnitude of k in the range $|k|' < 2$, e.g., throughout the range of interest. The structure function S has been averaged over all wave vectors having the same values of $|k|'$.

The error bars were deduced by assuming that for each trajectory the nonzero or imaginary parts of the Fourier transform of the concentration are Gaussian random variables. This is the expected result for sufficiently large systems since each Fourier component of the order parameter is the sum of a large number of essentially independent contributions from noninteracting patches. The central limit theorem[33] implies therefore that the sum is a Gaussian random variable. This

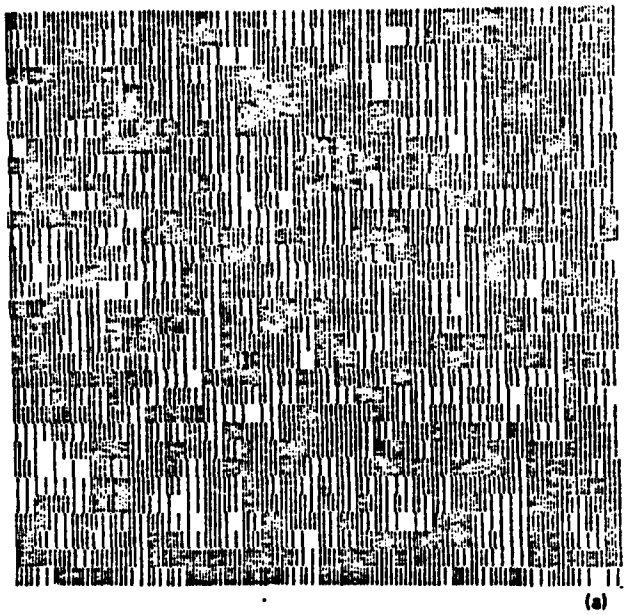

(a)

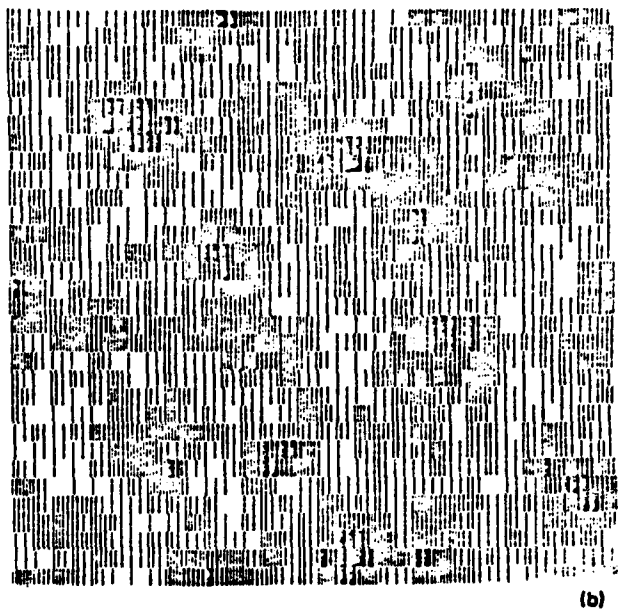

(b)

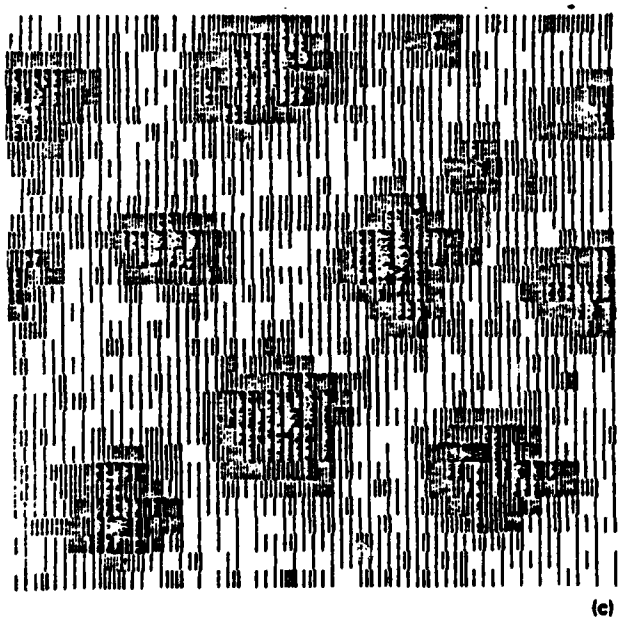

(c)

FIG. 2. Same as Fig. 1 but for an off-critical quench. The light squares are used for the majority phase.

argument, of course, fails for integrals over the Fourier components of the concentration, e.g., the concentration at a given point is not necessarily Gaussian. We have checked the above assumption by calculating, from the results of our simulation, the mean square fluctuation for the square of each Fourier component. We find no statistically significant deviations from Gaussian behavior.

In Figs. 4 and 5 we have shown the values of the structure function for various times during the decomposition. In these figures we have simply drawn smooth curves through plots similar to those in Fig. 3, consistent with the error bars. For these times we have not been able to find a convincing scaling form for the structure function as a function of some scaled wave vector.

It is also of interest to Fourier transform the structure factor and find the correlation function $S(|r|) = \langle c(r')c(r+r')\rangle$. This function is plotted in Fig. 6 for several times. It is interesting to note that $S(|r|)$ is a smooth function of the absolute value of the separation, for separations less than 16 lattice spacings (this is half way across the finite lattice). It therefore appears that the shape of the underlying square lattice is relatively unimportant to the structure function and we conjecture

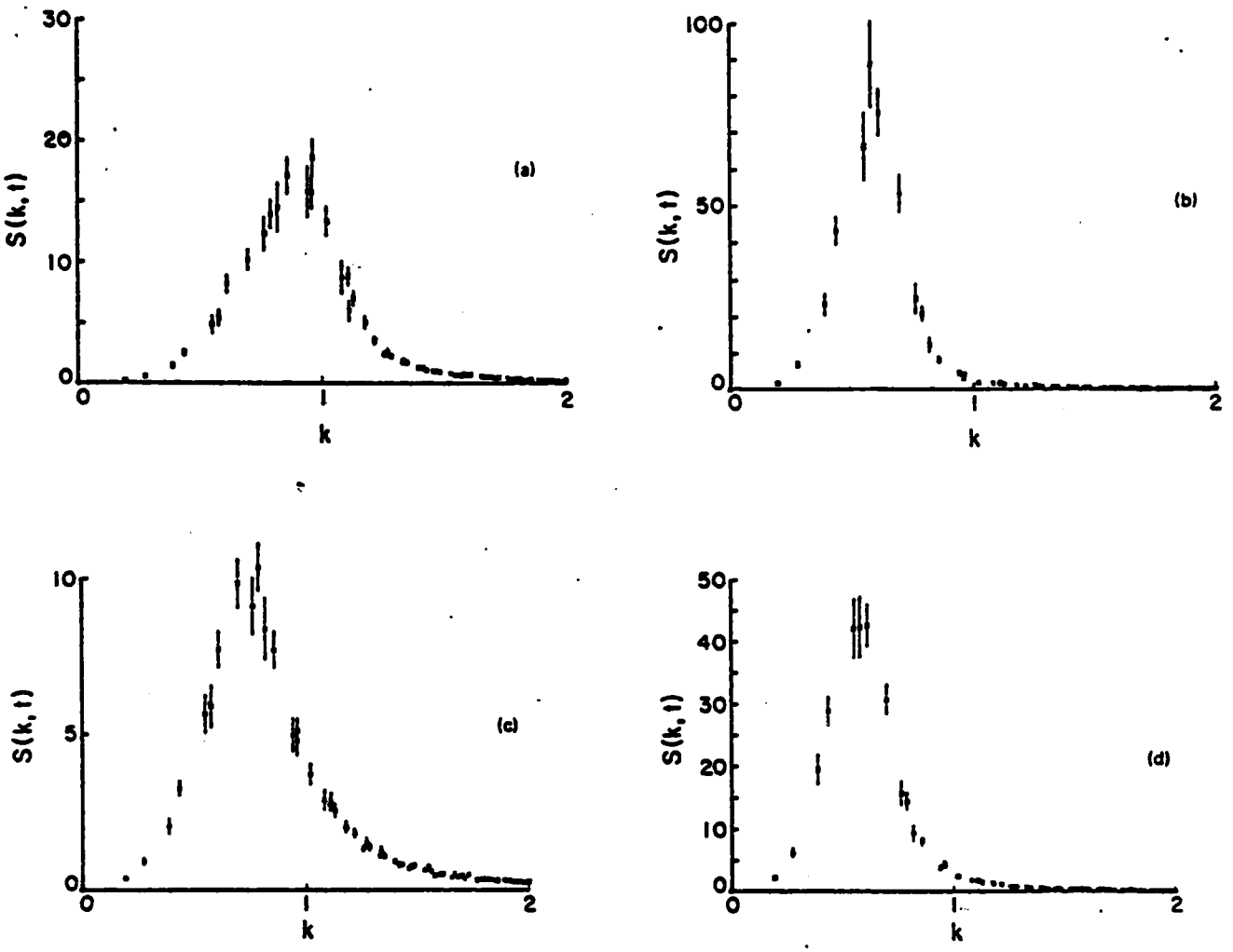

FIG. 3. The Fourier transform of the structure factor, $S(k,t)$ as a function of k, for several values of the time after the quench. (a) the critical quench, for $t = 38\ \tau_0$; (b) the critical quench, for $t = 223\ \tau_0$; (c) the off-critical quench for $t = 56\ \tau_0$; (d) the off-critical quench, for $t = 223\ \tau_0$. The (one standard deviation) error bars were estimated as discussed in the text.

that this is also relatively unimportant to the other quantities which we calculate. It is also interesting to note that the dependence of the structure function on $|r|$. The shape at small $|r|$ is easy to understand: nearby points tend to have similar values of the concentration. Because of the conservation law there is a sum rule ($\int dr\, S(r) = 0$) and therefore $S(|r|)$ must be negative at larger r. However we find a persistent peak at yet larger r which contributes appreciably to this sum rule. This is due to the relative sharpness of the peak in the structure function as a function of k. This suggests that some care should be taken in simulating spinodal decomposition to ensure that the system is large enough as spatial correlations persist appreciably further than the naive estimate π/k_{max}, where k_{max} is the location of the maximum in the structure function as a function of k at that time. Note that for the latest time for which we have data the second peak in the structure function is zero only at 15 lattice constants, essentially halfway across our finite lattice.

We have tested the validity of the linear theory at short times by comparing the results of our simulation to the linear equations for the structure factor. We find that after 0.5 and 1 linear growth times (i.e., $t/\tau_0 = 2$ or 4) the amplitude of the fastest growing linear mode already exceeds by a factor of 2 that given by the full nonlinear simulation.

It is interesting to ask whether or not this disagreement between the results of the computer simulation and the linear theory can be explained simply by the random phase approximation (RPA) theory for the interactions between the quickly relaxing high k modes and the more slowly relaxing k modes. In RPA the rate of change of the structure function is given by[20]

$$\frac{dS(k)}{dt} = 2M|k|^2[(|k|^2 + a_{RPA})S(k) + 1]\,, \tag{21}$$

where

$$a_{RPA} = a + 3u\,S(r=0)\,. \tag{22}$$

Rather than solving these equations and comparing the results to those of the computer simulation we have

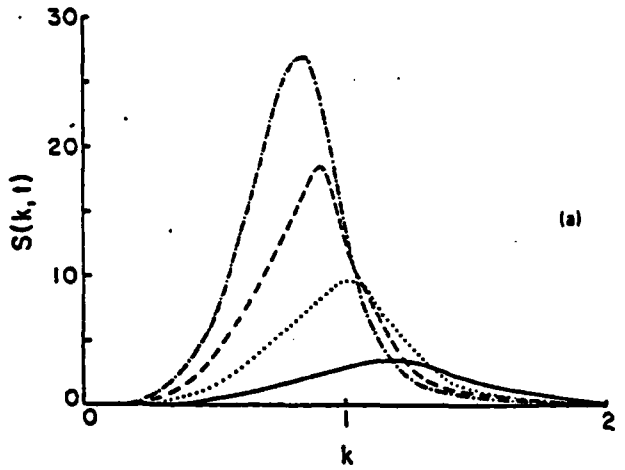

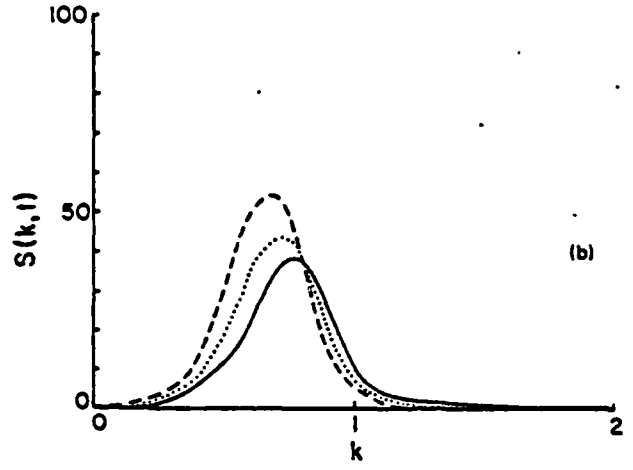

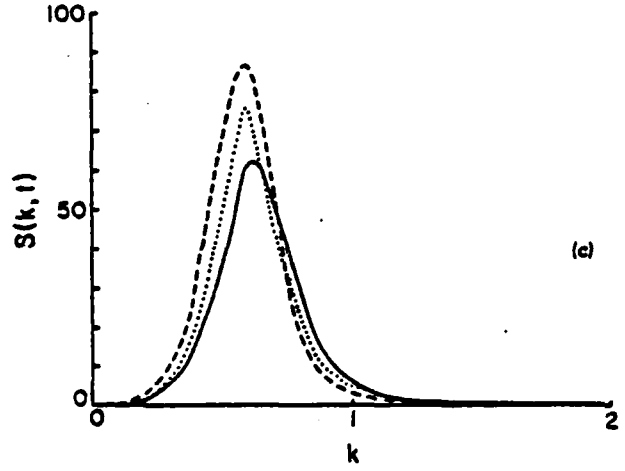

FIG. 4. A plot of the structure factor $S(k,t) = K \langle |c(k,t)|^2 \rangle (Nk_BT)^{-1}$ as a function of k. The value of k is computed as described in Sec. II B. The curves were visually smoothed out, consistent with the estimated error bars. (a) Represents $S(k,t)$ for a critical quench and various times: $t = 10\ \tau_0$, a solid line; $t = 23\ \tau_0$, a dotted line; $t = 38\ \tau_0$, dashed line; $t = 56\ \tau_0$, a dot–dashed line. (b) Represents $S(k,t)$ for a critical quench for various times: $t = 77\ \tau_0$, a solid line; $t = 100\ \tau_0$, a dotted line; $t = 127\ \tau_0$, a dashed line. (c) Represents $S(k,t)$ for a critical quench, at various times: $t = 156\ \tau_0$, a dotted line; $t = 100\ \tau_0$, a dotted line; $t = 223\ \tau_0$ a dashed line.

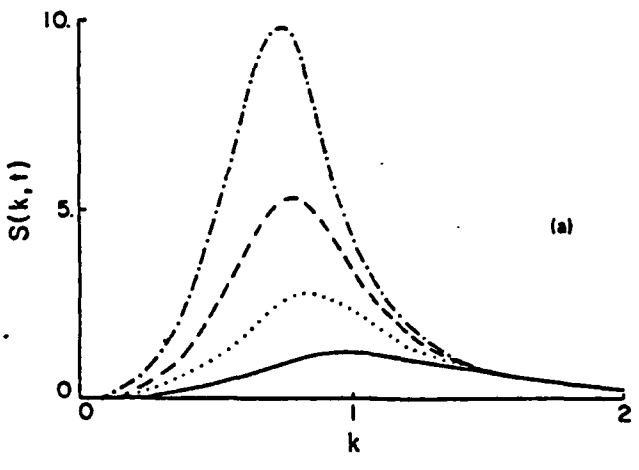

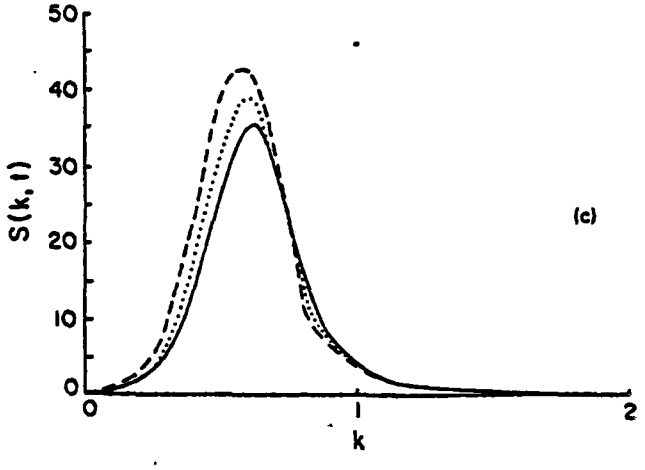

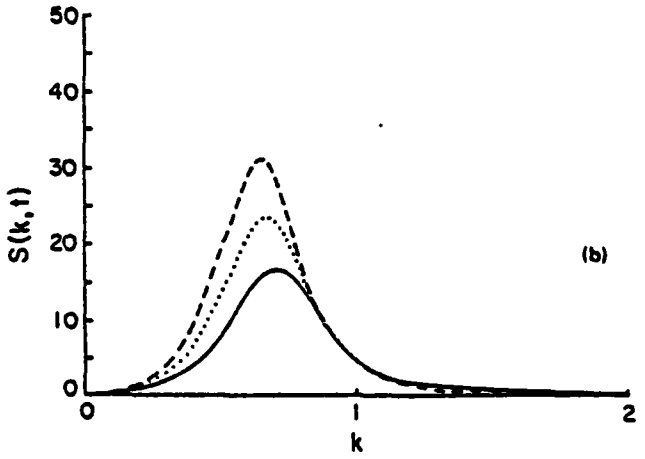

FIG. 5. Same as Fig. 4, but for the off-critical quench.

chosen to examine the computer simulation to see when the assumptions of the RPA theory break down. It seems reasonable to assert that this breakdown will be less dependent on the choice of initial state (which is not easily controllable in real experiments) than the detailed mean field theory dynamics.

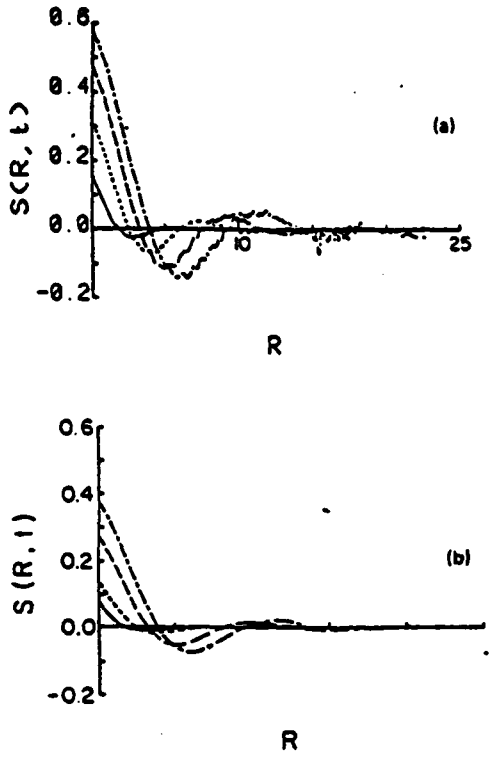

FIG. 6. The structure factor $S(|r|,t)$ as a function of $|r|$, at various times after the quench. (a) The critical quench: $t = 10\,\tau_0$, a solid line; $t = 38\,\tau_0$, a dotted line; $t = 100\,\tau_0$, a dashed line; $t = 223\,\tau_0$, a dot–dashed line. (b) Same as (a), but for the off-critical quench.

In particular, underlying the RPA assumptions is that the fluctuations in $c(r)$ are Gaussian (like in the linear model, but with the width renormalized by fluctuations). In Fig. 7 we give plots of $\langle c(r)^4\rangle - 3\,\langle c(r)^2\rangle^2$. For the off-critical quench we have also given $\langle c^3\rangle$; for a critical quench our free energy functional gives $\langle c^3\rangle = 0$. If the fluctuations are Gaussian both $\langle c^4\rangle - 3\,\langle c^2\rangle^2$ and $\langle c^3\rangle$ are zero and the non-Gaussian nature of the fluctuations can be deduced from the dimensionless ratios $(\langle c^4\rangle - 3\,\langle c^2\rangle^2/\langle c^2\rangle^2$ and $\langle c^3\rangle/\langle c^2\rangle^{3/2}$. The graphs show that the fluctuations become non-Gaussian quite early in the decomposition, indicating that nonlinear effects reach quickly beyond the behavior implied by the random phase approximation.

It is difficult to assess *a priori* the statistical uncertainty in the one-point moments discussed above or in various other quantities which are discussed below. This is because the statistical distribution of such quantities at a single point is a complex dynamical quantity and because all such quantities were averaged over all the sites in the lattice. Thus, these quantities are the sum of a large number of statistically *dependent* variables with distributions and correlations which are not known *a priori*. Some idea of the accuracy of these moments can be obtained by calculating the value of moments such as $\langle c(r)^3\rangle$, which are required by symmetry to be zero in the critical quench. Such tests suggest that the statistical accuracy of these moments and those discussed below are of order 3%.

3. *The distribution functions*

Another quantity of interest is the one particle distribution function $P_1(c,t)$ defined in Sec. IIC. This is the probability that the concentration at an arbitrary cell has the value c at time t. Numerical results for $P_1(c,t)$ as a function of c, at various times, are displayed in Figs. 8 and 9. The initial distribution ($t = 0$) has nonzero value for $c = c_0$ only, since this our initial condition. At later times the distribution broadens and then starts to develop two peaks near the mean-field equilibrium values. For $c_0 = 0$ (Fig. 8) the distribution is symmetric with respect to 0. As the time evolves the number of cells having the initial concentration is substantially diminished and the peak values become more and more probable. In other words more cells tend to have the concentration near the mean-field equilibrium values.

In the very long time limit, when the system reaches equilibrium we expect that $P_1(c;t\to\infty)$ consists of a sum of two nearly Gaussian distributions centered around

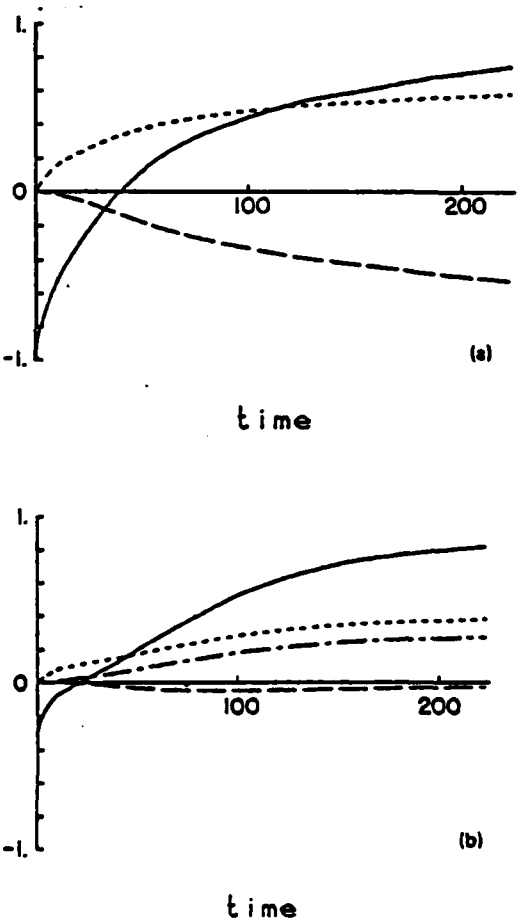

FIG. 7. We show here the dependence of time of various quantities related to the RPA approximation (see the text). (a) For a critical quench we have: Full line: We plot a_{RPA} given by Eq. (22); dotted line: We plot $\langle |c(R,t)|^2\rangle/C_{eq}^2$, as a function of time; dot–dashed line. We plot $\langle c(R,t)^3\rangle/C_{eq}^3$, as a function of time; dashed line: We plot $(\langle c(R,t)^4\rangle - 3\,\langle c(R,t)^2\rangle^2)/C_{eq}^2$, as a function of time. (b) Same as (a), but for the off-critical quench. The mean field value of C_{eq}, defined in Eq. (17), was used.

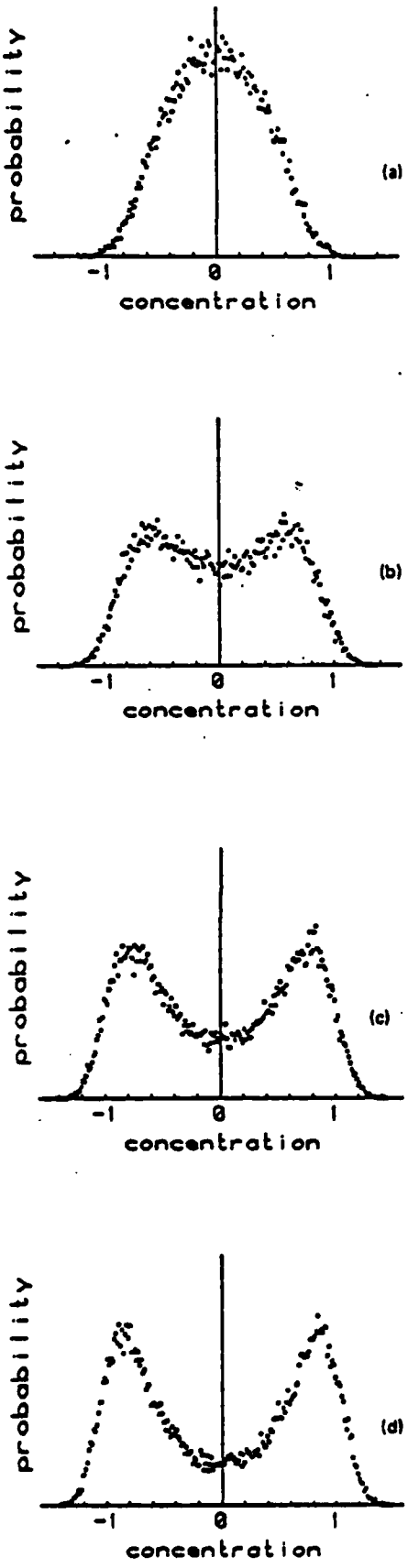

FIG. 8. The probability $P(c,t)$ of finding the concentration c, in a cell at the time t after a critical quench. (a) $t = 10\ \tau_\phi$; (b) $t = 38\ \tau_\phi$; (c) $t = 223\ \tau_\phi$. See the text for a discussion of the definition of P.

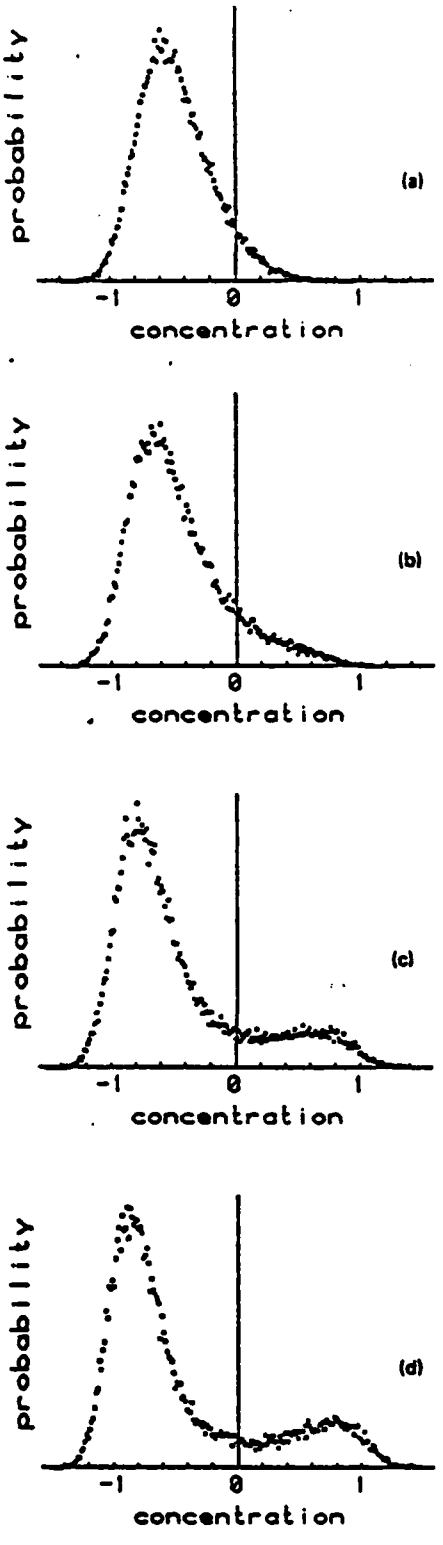

FIG. 9. Same as Fig. 8, but for the off-critical quench.

the actual equilibrium concentrations, each Gaussian having a width given by $\int S_{eq}(k)dk$ where $S_{eq}(k)$ is the equilibrium value of the concentration correlation function in the corresponding phase. We have tried to fit $P_1(c,t)$ at earlier times with such a double Gaussian form and were *quantitatively* unsuccessful.

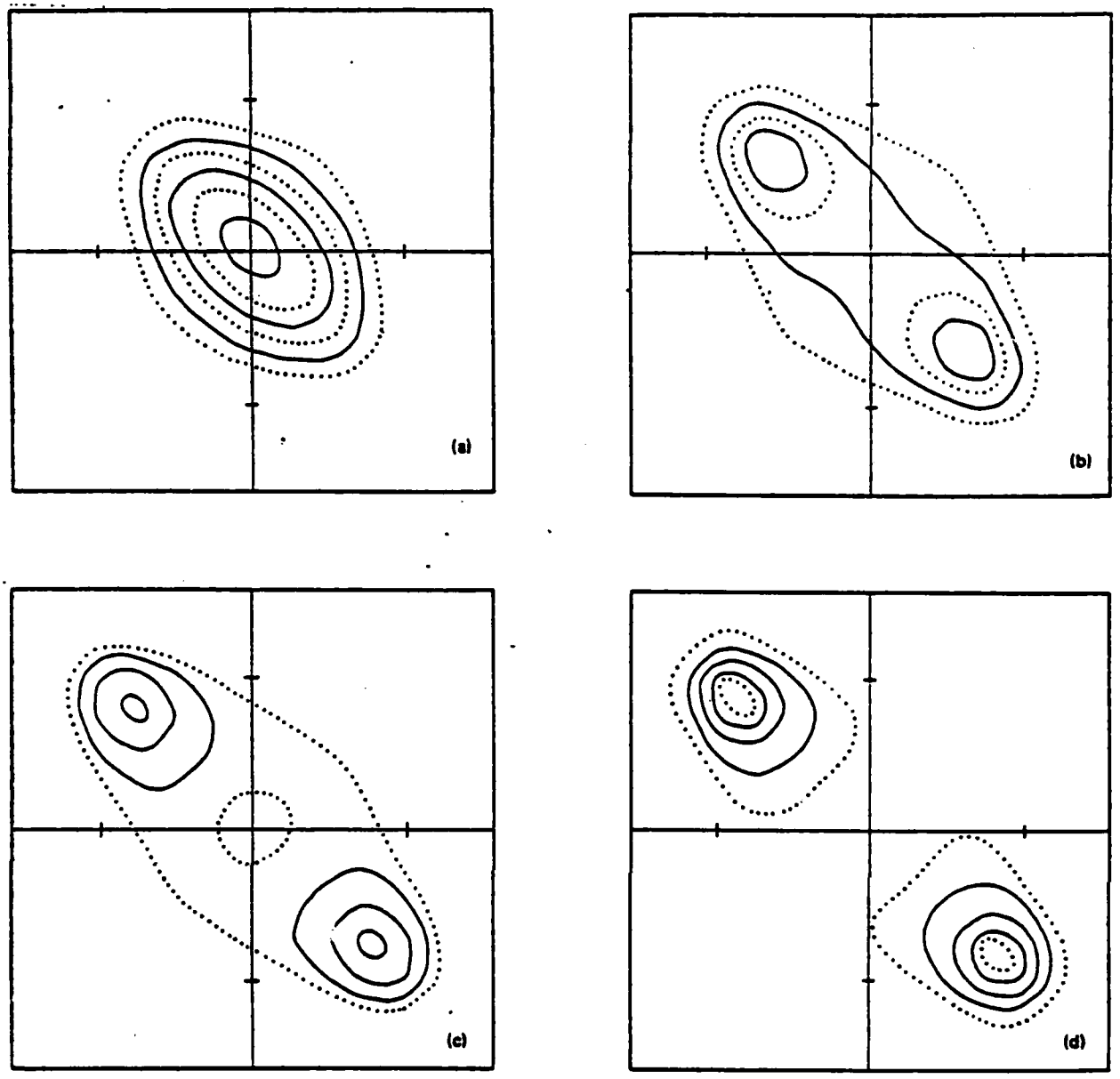

FIG. 10. Contour plots of the two-point probability distribution $P_2(c_1, c_2; t)$, representing the probability that at time t the concentration in one cell is c_1 and that in a nearest neighbor is c_2. The axes represent the values of c_1 and c_2. The tick marks represent the mean field values of C_{eq}. The solid lines are lines of constant probability drawn at equally spaced intervals $[P(c_1, c_2) = \Delta P\, n;\ n \text{ integer}]$. Dotted lines have been drawn at intermediate intervals $[P(c_1, c_2) = \Delta P(n + 0.5)]$ in regions where the contours are widely spaced. The value of ΔP was $0.62\ C_{eq}^2$. This has been done at several times; (a) $t = 10\ \tau_\theta$; (b) $t = 38\ \tau_\theta$; (c) $t = 100\ \tau_\theta$; (d) $t = 233\ \tau_\theta$.

We have also computed the two-point probability distribution function $P_2(c_i, c_j; t)$ defined in Sec. II C. This is the probability that, at time t, the concentration in the cell i is c_i and that in cell j is c_j. In Figs. 10 and 11 we show contour plots joining the points (c_i, c_j) of equal probability. This should be read as a topographic map in which the surface of the "mountains" is $P_2(c_i, c_j; t)$, at fixed t. In Figs. 10(a)–10(d) we present the case when i and j are nearest neighbors.

The symmetry of these figures under the exchange $c_1 \leftrightarrow c_2$ is a consequence of the definition of P_2. The symmetry under $c_1 \leftrightarrow -c_1$, $c_2 \leftrightarrow -c_2$ exists only in a critical quench for a free energy functional which is unchanged by $c \leftrightarrow -c$.

Note that for nearest neighbors the probability that one cell is near one equilibrium concentration and that a neighboring cell is at the other equilibrium concentration is relatively small. This shows that the incipient domain walls separating the areas of different phases are large compared to lattice spacing. If this were not the case we would expect the dynamics to depend on the underlying lattice.

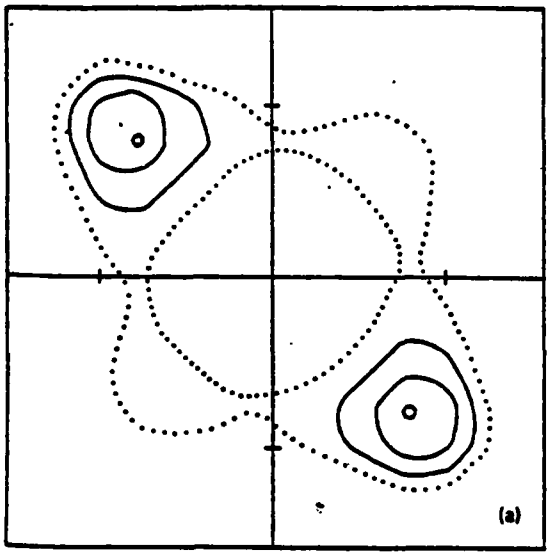

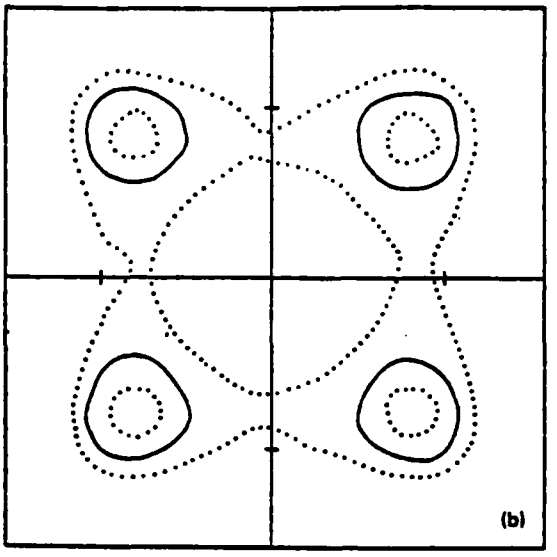

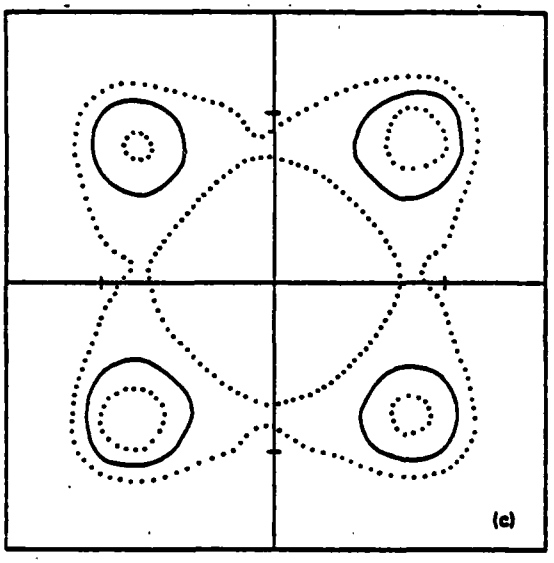

FIG. 11. In this figure we have given contour plots of the two-point probability distribution for a number of pairs of cells with different separations at the time 233 τ_0 (the latest time shown in Fig. 10). A description of these plots is given in the caption to Fig. 10, as is a plot for nearest neighbor pairs [Fig. 10(d)] at this time. The pairs of cells in these plots were separated along the x or y axes of the computer simulation by distances of 2 [Fig. 11(a)], 4 [Fig. 11(b)], and 8 [Fig. 11(c)] lattice spacings.

Note also the formation between the second and third times of a minimum in the distribution function near $c_1 = c_2 = 0$.

In Figs. 11(a)–11(c) we have shown the two-point probability for a number of different separation, for a critical quench, at the latest time we have simulated.

Contour plots for an off critical quench have similar features. However, they are difficult to read due to the very large probability that both points have concentrations near that of the majority phase and are not reproduced here.

It is important[20,22] to have a good description of this two-point correlation function in terms of a small number of parameters. A comparison of various parameterizations which have been used in theoretical work with the actual measured distributions is currently in progress.

ACKNOWLEDGMENTS

This work has been supported in part by the Office of Naval Research. We are grateful to Doug Scalapino, Susan Hill, Paul Meakin, Jim Langer, and David Cannell for useful discussions.

[1] J. Cahn, Metall. Soc. A.I.M.E. 242, 166 (1968).
[2] J. S. Langer, in *Fluctuations, Instabilities and Phase Transitions*, edited by T. Riste (Plenum, New York, 1975).
[3] H. Metiu, K. Kitahara, and J. Ross, in *Fluctuation Phenomena*, edited by E. W. Montroll and J. L. Lebowitz (North-Holland, New York, 1979).
[4] F. F. Abraham, Phys. Rep 53, 95 (1979).
[5] K. B. Rundman and J. E. Hilliard, Acta Metall. 15, 1025 (1967); S. Agarwal and H. Herman, Scr. Metall. 7, 503 (1973); R. Alcuña and A. Bonfiglio, Acta Metall. 22, 399 (1974); V. Gerold and W. Mertz, Scr. Metall. 1, 33 (1967);

T. L. Bartel and K. B. Rundman, Metall. Trans. 6, 1887 (1975); Y. E. Hilliard and K. B. Rundman Scr. Metall. 1, 37 (1967).
[6]G. T. Feke and W. Prins, Macromolecules 7, 527 (1974).
[7]G. F. Neilsen, Phys. Chem. Glasses. 10, 54 (1969); M. Tomozawa, R. K. McCrone, and H. Herman, J. Am. Ceram. Soc. 55, 62 (1970); N. S. Andreev, G. G. Boiko, and N. A. Bokov, Noncryst. Solids 5, 41 (1970).
[8]J. S. Huang, W. I. Goldburg, and A. W. Bjerkaas, Phys. Rev. Lett. 29, 921 (1974); A. J. Schwartz, J. S. Huang, and W. I. Goldburg, J. Chem. Phys. 62, 1847 (1975); N. Wong and C. M. Knobler, *ibid.* 66, 4707 (1977).
[9]J. W. Cahn, Acta. Metall. 9, 795 (1961); 10, 179 (1962).
[10]H. E. Cook, Acta. Metall. 18, 297 (1970).
[11]J. S. Langer, Ann. Phys. N.Y. 54, 258 (1969); 65, 53 (1971).
[12](a) H. Metiu, K. Kitahara, and J. Ross, J. Chem. Phys. 65, 393 (1976); (b) 63, 5116 (1975).
[13]P. C. Hohenberg and B. I. Halperin, Rev. Mod. Phys. 43, 435 (1977).
[14]J. D. van der Waals, Z. Phys. Chem. (Leipzig) 28, 258 (1894).
[15]J. W. Cahn and J. E. Hilliard, J. Chem. Phys. 28, 258 (1958).
[16]V. L. Ginzburg and L. D. Landau, Zh. Eksp. Teor. Fiz. 20, 1064 (1950).
[17]K. G. Wilson, Phys. Rev. Lett. 28, 580 (1972); K. G. Wilson and J. Kogut, Phys. Rep. 12, 75 (1974).
[18]J. S. Langer, Physica (Utrecht) 73, 61 (1974).
[19](a) S. K. Ma, *Modern Theory of Critical Phenomena* (Benjamon, Reading, Mass, 1976). (b) D. J. Amit, Field Theory, *The Renormalization Group and Critical Phenomena* (McGraw-Hill, New York, 1978).
[20]J. S. Langer, M. Bar-on, and H. O. Miller, Phys. Rev. A 11, 1417 (1975).
[21]K. Kawasaki and T. Ohta, Prog. Teor. Phys. 59, 362 (1978).
[22]S. C. Hill, H. Metiu and R. G. Petschek (unpublished).
[23]It is hoped that ongoing experiments carried out by D. S. Cannell and C. M. Jefferson with a mixture 3-methylpentane-nitroethane in which the refractive indices of the components are nearly equal, will provide data free of multiple scattering.
[24]W. I. Goldburg and J. S. Huang, in *Fluctuations, Instabilites and Phase Transitions*, edited by T. Riste (Plenum, New York, 1975).
[25]J. Bohr, M. Nielsen, J. P. McTague, J. Als-Nielsen, and K. Kjaer (preprint).
[26]For a phase diagram see J. A. Safran, Phys. Rev. Lett. 44, 937 (1980); Dr. Safran has suggested that spinodal decomposition might take place in intercalated compounds (private communication).
[27]A. B. Bortz, M. H. Kalos, J. L. Lebowitz, and M. A. Zendejas, Phys. Rev. B 10, 535 (1974); J. Marro, A. B. Bortz, M. H. Kalos, and J. L. Lebowitz, *ibid.* 12, 2000 (1975); M. Rao, M. H. Kalos, J. Marro, and J. L. Lebowitz, *ibid.* 13, 4328 (1976); A. Sur. J. L. Lebowitz, J. Marro, and M. H. Kalos, *ibid.* 15, 3014 (1977).
[28]M. R. Mruzik, F. F. Abraham, and G. M. Pound, J. Chem. Phys. 69, 3462 (1978).
[29]It is implicitly assumed in Eq. (4a) that the coexistance line is symmetric with respect to T_c. This is generally true for concentration close to c_c. This assumption can be easily removed.
[30]H. Metiu (unpublished).
[31]R. Petschek and H. Metiu (to be published).
[32]H. Guttinger and D. S. Cannell, Phys. Rev. A 6, 3188 (1981).
[33]A. I. Khinchin, *Mathematical Foundation of Statistical Mechanics* (Dover, New York, 1949), Chap. V.

Scholar.

note the difference between the concentration, denoted

END

FILMED

8-83

DTIC